ZnO Deposit on O-ZrP as Paper Filler and its Potential Antibacterial Property

Zhihan Li, Rendang Yang, Fei Yang, Ming Zhang, and Bin Wang*

ZnO nanoparticles (NPs) were reduced by treatment with chitosan oligosaccharide (COS) and loaded on organic zirconium phosphate (OZrP) by electrostatic self-assembly in an aqueous medium. The size and morphology of the ZnO NPs was modified using OZrP, which was applied to disperse the ZnO NPs and act as a stabilizer. The synthesized nanocomposites (NC) were used as fillers, and the surface coating method was applied to prepare cellulose-based composite papers having antibacterial properties. The composites were characterized using UV/vis spectroscopy, transmission electron microscopy (TEM), energy dispersion X-ray (EDX) spectrometry, X-ray diffraction (XRD), zeta potential measurements, and scanning electron microscope (SEM). Results indicated that the average diameter of ZnO NPs was less than 50 nm. ZnO NPs was dispersed on the surface and in the interlayer of the OZrP. The physical properties of the finished papers were improved by coating with ZnO/COS/OZrP (ZCO) NCs. Paper that was coated with ZCO yielded good antibacterial properties.

Keywords: ZnO nanoparticles; Chitosan oligosaccharide; Organic zirconium phosphate; *Antibacterial paper; Packaging application*

*Contact information: State Key Laboratory of Pulp & Paper Engineering, South China University of Technology, Guangzhou 510640, China; *Corresponding author: febwang@scut.edu.cn*

INTRODUCTION

Cellulosic materials obtained from plants available in forests and also grown through agriculture are considered renewable resources (inexhaustible resources) for use in the production of paper and paperboard (Liu *et al*. 2013). Paper is the most widely used material in packaging applications, owing to its characteristics of printability, biodegradability, renewability, recyclability, mechanical flexibility, and affordability (Hubbe and Bowden 2009; Nassar and Youssef 2012). However, cellulose does not have any antimicrobial activity, and most molds or bacteria can multiply rapidly on cellulosic paper under the proper conditions. Therefore, inorganic and natural antibacterial materials have been studied and widely used for the packaging paper process (Chan *et al*. 2011; Manna *et al*. 2015). Among the metal oxide antibacterial agents, ZnO has aroused concern due to its ability for killing Gram positive and Gram negative bacteria, as well as inhibiting the growth of fungi (Shah *et al*. 2014; Diez-Pascual *et al*. 2014).

Nanotechnology has allowed paper technologists to produce multifunctional paper products (Fu *et al*. 2015). When nanometals, *e.g.,* ZnO, are incorporated into the paper matrix, antibacterial properties are acquired.

In addition to the antimicrobial activity, structural integrity (strength) is also an important attribute for food packaging paper. In recent years, many researchers have focused on the water-soluble chitosan oligosaccharide (COS), a relatively low molecular weight compound (Liu *et al*. 2014). In order to promote ionic interactions with the negatively charged components of the bacterial cell membrane, the incorporation of metal oxide has also been reported recently as an alternative approach (Krishna Rao *et al*. 2014). Consequently, COS has reactive amino and hydroxyl groups that could be used as a reducing agent in the process of metal NP preparation (Anandhavelu and Thambidurai 2012).

The α-zirconium phosphate (ZrP) material is favorable for use in paper products because of its ability to serve as an ion exchanger, reaction catalyst, and carrier of intercalation (Wu *et al*. 2014). With a self-organized lamellar structure and abundant hydroxyl group, ZrP has the potential to be used as a stabilizer for NPs.

However, to the best of our knowledge, there has been no research reporting on the design of antibacterial, paper-based ZrP nanocomposites (NC) in which tailored materials, such as ZnO NPs and chitosan oligosaccharide, were chosen. In this work, COS can be considered as a reducer, and OZrP was expected to be a growth template and further a stabilizer for ZnO NPs. Then, ZnO/COS/OZrP (ZCO) NCs were coated onto papers to obtain antibacterial properties.

EXPERIMENTAL

Materials

Chitosan oligosaccharide (molecular weight: 2 kDa, DD ⩾ 95.0% according to the manufacturer) was purchased from Hedebei Ocean Biochemical Co. Ltd. (Shandong, China). Zirconium oxychloride octahydrate ($ZrOCl2 \cdot 8H2O$, 98%) and zinc acetate were obtained from Sigma-Aldrich (Shanghai, China). Hexadecyl trimethyl ammonium Bromide (CTAB) was purchased from Sinopharm Chemical Reagent Co., Ltd. (Shanghai, China).

Escherichia coli (ATCC8739), *Staphylococcus aureus* (ATCC6538), *Aspergillus niger* (ATCC16404), and *Bacillus subtilis* (ATCC6633) were provided by the Guangdong Institute of Microbiology, Guangdong, China. *Eucalyptus* bleached chemi-mechanical pulp (BCTMP) was supplied by the Shandong Huatai Paper Co., Ltd., Dongying, China.

All aqueous solutions were prepared with ultrapure water (>18 MΩ cm) from a Milli-Q Plus system (Millipore, USA).

Methods

Preparation of OZrP

The ZrP was synthesized using previously reported methods (Maclachian and Morgan 1992). The cation exchange capacity (CEC) of ZrP was measured using the NH_4Cl-CH_3CH_2OH method (Wu *et al*. 2014). It was calculated that the CEC of ZrP was approximately 196 mmol/100g. The OZrP was prepared as follows: ZrP (4.0 g) was dispersed in ultrapure water and stirred at 200 rpm/min at 50 °C for 1 h. After adding a

desired amount of CTAB (1.092 g, 0.5 CEC), the reaction mixture was stirred for 5 h at 50 °C. The products were centrifuged, washed repeatedly with ultrapure water, dried at 60 °C, grounded in an agate mortar, and passed through a 200-mesh sieve.

Preparation of ZCO NCs

The ZnO NPs were prepared *via* hydrothermal reduction processing. A $Zn(CH_3COO)_2$ solution (50 mL, 1 mg/mL) was added to the solution of COS (50 mL, 2 mg/mL) in a 250-mL glass flask, which was kept in a water bath and connected to a condenser. Then a required amount of OZrP was added to the mixed solution. Subsequently, the reaction mixture was stirred with a magnetic stir bar for 6 h at 60 ^oC Composites of ZCO NCs were prepared by electrostatic assembly in an aqueous medium, using polyelectrolytes as the macromolecular linkers. Two kinds of ZCO NCs were prepared by controlling the ratios of COS to OZrP to zinc acetate; these ratios were 100 mg: 50 mg: 50 mg (ZCO-1) and 100 mg: 50 mg: 100 mg (ZCO-2), respectively. The final samples were labeled as ZCO-1 and ZCO -2.

Application of coating antibacterial paper

The aspen BCTMP was placed into a fiber mill beater (Mark V1-PFI, Norway) at 2000 r/min until the beating degree reached 40° SR. The paper sheets were prepared according to the TAPPI Standard T205 sp-02 (2002), using the model Rapid-Koethen sheet former (RK3AKWT, Sweden) with a target basis weight of 70 g/m^2. Then, ZCO of different concentrations (*i.e.*, 0.5, 1.0, 1.5, 2.0, and 2.5 wt%) were dispersed in water and coated uniformly on the paper surface with the use of a coating machine (Auto bar coater, PIT, Germany). Finally, the dried paper was cut into square pieces for subsequent physical property analysis and antibacterial experiments.

Characterization

The UV-spectroscopy was recorded on a UV-240 spectrophotometer (Shimadzu, Japan). The morphological nanostructure of the ZnO-NPs and ZCO NCs were elucidated by transmission electron microscope (TEM; JEOL, Japan) with an acceleration voltage of 200 kV. The zeta potential of the ZnO-NPs, ZrP, OZrP, and ZCO NPs suspensions was measured using a Zetasizer Nano ZS instrument (Malvern Instruments Ltd., UK). The energy dispersive X-ray (EDX) spectra were recorded with an Oxford ISIS-300 EDX spectrometer. X-ray diffraction (XRD Bruker AXS, Germany) patterns were obtained using a D8 advanced X–ray diffractometer (40 kV, 50 mA) with Cu Kα radiation (λ = 0.15418 nm), a scattering range of 1° to 10° and 5° to 80° (2θ), and a scanning rate of 1°/min and 10°/min, respectively. The surface morphology of the antibacterial papers was obtained using a Zeiss EVO18 scanning electron microscope (SEM; Germany).

Antibacterial activity

The test was carried out using an antimicrobial method on agar plates. To examine the antibacterial effect of ZCO NC-coated paper, *Escherichia coli* (ATCC8739), *Staphylococcus aureus* (ATCC6538), *Aspergillus niger* (ATCC16404), and *Bacillus subtilis* (ATCC6633) were used as the test organisms. The bacteria were grown in nutrient bouillon medium (18 g/L nutrient bouillon and pH 7.0) for 12 h at 37 °C, and

further diluted to achieve a concentration of about 10^4 CFU/mL with aseptic water. Then, the diluted suspensions (0.1 mL) of *bacteria* were distributed into the LB agar medium using 18 g/L nutrient bouillon and 15 g/L agar. Samples of the antimicrobial papers, which had been autoclaved, were placed on the nutrient medium with individual test microorganisms. After the plates were incubated at 37 °C for 24 h for the bacteria and at 30 °C for 48 h for *Aspergillus niger*, the zones of inhibition were observed. The papers without the antimicrobial agents served as the control samples. All of the data were reported as the mean value of three parallel experiments; the discrepancies among them were less than 5%.

Physical properties

The finished paper samples were stored in a conditioning room with a temperature of 25 ± 1 °C and a relative humidity of 50% ± 2 for 24 h. The tensile, tear, bursting strengths, and brightness were measured according to the ISO 1924 (2008), ISO 1974 (2012), ISO 2758 (2001), and TAPPI T452 (1998) standards, respectively, using Lorentzen and Wettre (L & W) tensile testers (Sweden), L & W tear testers, a L & W Burst-O-Matic, and a L & W digital ISO brightness meter, respectively. All of the experiments were triplicates and the data was averaged.

RESULTS AND DISCUSSION

Preparation and Characterization of ZnO NPs

The UV-visible spectra of ZnO NPs prepared with different concentrations are shown in Fig. 1. The absorption peaks of ZnO NP-1 and ZnO NP-2, which are at approximately 370 nm. When the ZnO NPs were synthesized from the different ratios of COS and zinc acetate, the particle size was slightly smaller than the others, and their quantum size effect changed. Thus, the band gap marginally decreased.

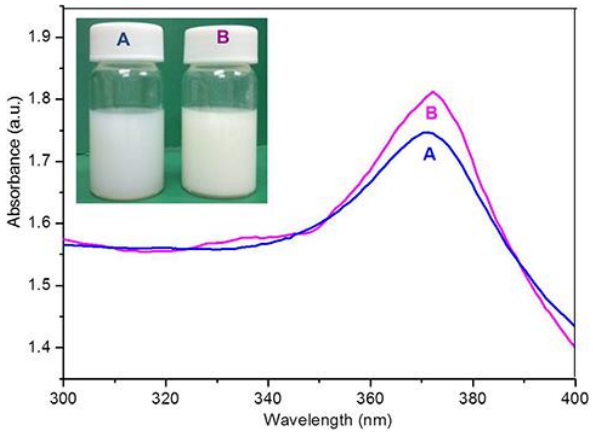

Fig. 1. UV−visible spectra of ZnO NPs prepared in aqueous solutions at two different molar concentrations of $Zn(CH_3COO)_2$: (A) 0.265 mmol and (B) 0.530 mmol. The inset shows photographs of the solutions containing ZnO NPs synthesized with different molar concentrations of $Zn(CH_3COO)_2$ represented by (A) ZnO (0.265 mmol) NPs and (B) ZnO (0.530 mmol) NPs

The micrographs of the ZnO NPs prepared at different molar concentrations are shown in Fig. 2. The TEM images indicate that the ZnO NPs prepared at different concentrations of zinc oxalate were nearly polygonal in shape. Figure 2a revealed that the NPs were composed from irregular shape particles, with an average particle size of approximately 50 nm. There were no noticeable changes in the mean size with increasing molar concentrations of reagents in Fig. 2b. A comparison between Fig. 2a and 2b indicated that the initially higher concentrations of zinc chloride produced more zinc oxide NPs. All of the ZnO NPs were evenly distributed, without forming agglomerates. The results suggested that the interactions between the −OH groups of the ZnO surface and the $-NH_2$ moieties of the COS prevented NP aggregation. As shown in Fig. 2c and 2d, all of the ZnO NPs were thoroughly dispersed on the surface and in the interlayer of the OZrP. Therefore, using ZnO NPs and COS as coating agents was an efficient way to suppress agglomeration on the deposited template.

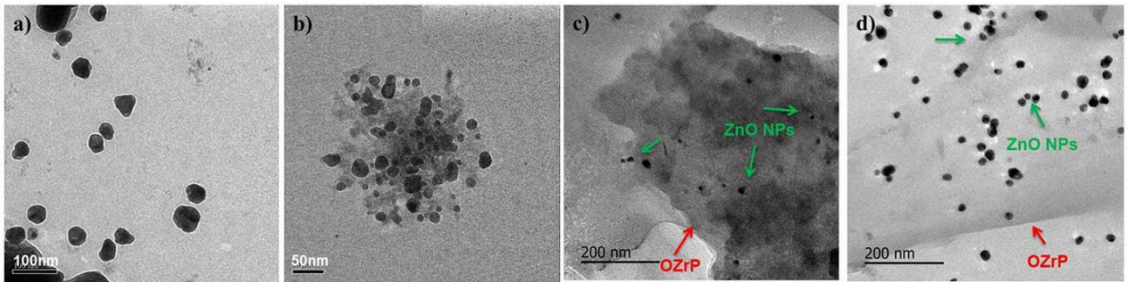

Fig. 2. TEM micrographs of ZnO NPs prepared in aqueous solutions at two different molar concentrations of $Zn(CH_3COO)_2$:(a) 0.265 mmol and (b) 0.530mmol; (c) ZCO-1 NCs and (d) ZCO-2 NCs

Properties of ZCO NCs

The XRD patterns are presented in Fig. 3a and 3b. For ZrP, a typical diffraction peak at 11.71° corresponded to a basal spacing (d002) of 0.76 nm in Fig. 3b (Maclachian and Morgan 1992). In order to increase the layer spacing, ZrP was firstly intercalated by CTAB. As shown in Fig. 3a, the diffraction peaks emerged at the lower 2θ value of 2.76°, corresponding to the increased d002 basal spacing of 3.20 nm. The results implied that the cationic surfactant was intercalated into the interlayer of ZrP, which increased the interlamellar spacing of ZrP. As for ZCO-1, a new peak was formed at the 2θ value of 1.74°, corresponding to the d002 basal spacing of 5.07 nm (Fig. 3a). This may have resulted from the intercalation of COS and ZnO NPs into the layer spacing of OZrP. The new diffraction peaks in Fig. 3b at the 2θ values of 31.7°, 34.4°, 36.2°, 47.5°, 56.5°, 62.8°, 66.3°, and 67.9°corresponded to the (100), (002), (101), (102), (110), (103), (200), and (112) planes of ZnO, respectively, and can readily be indexed to the hexagonal zincite (Sun *et al*. 2014).

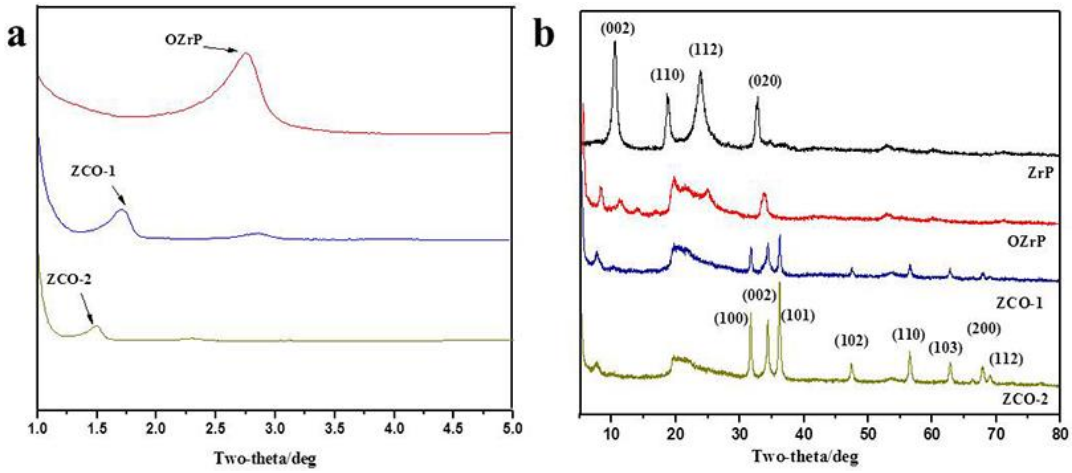

Fig. 3. (a) Small-angle and (b) wide-angle XRD patterns of ZrP, OZrP, and ZCO NPs

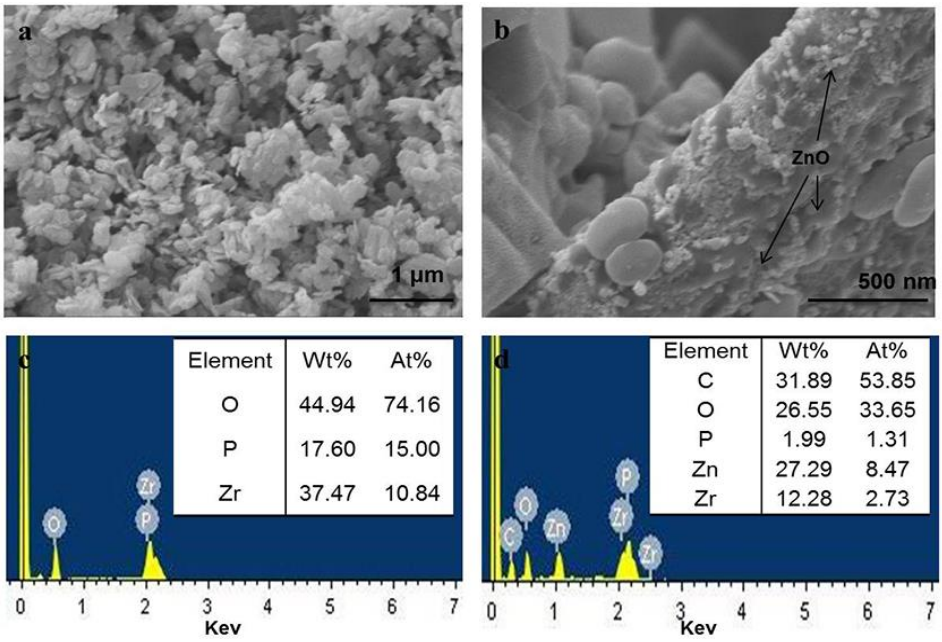

Fig. 4. SEM micrographs of (a) ZrP and (b) ZCO-2; EDX spectra of (c) ZrP and (d) ZCO-2

The morphology of the ZrP NPs was characterized using SEM, as shown in Fig. 4a. The image indicates that the ZrPs were made up of aggregated polygon plates and that the disks had well-defined shapes and smooth surfaces. The morphology of the solid layers was arranged in parallel, showing good crystallinity, and typical morphology for layered compounds. Figure 4c shows the EDX spectrum of ZrP, revealing that the ZrP contained elements of O, P, and Zr, which meant that the compound, α-$Zr(HPO_4)_2$•H_2O, was present (Wu *et al*. 2014). The representative SEM image of ZCO-2 is shown in Fig. 4b. The ZCO exhibited a mass of particles on the surface of OZrP. It was observed that the ZnO NPs were dispersed on the surface of OZrP. Fig. 4d shows the EDX spectrum of ZCO-2, revealing that ZCO-2 contained elements of C, O, P, Zr, and Zn. The presence of

Zn corroborated the existence of ZnO NPs, and that the elemental C could have been derived from COS. In this novel, multifunctional, NC, the inorganic carrier is a filler, which exhibits a twofold advantage: it serves as a ZnO NP supporting material for a slow and sustained release of ZnO in an aqueous medium, and it offers better performance to the paper product, such as dimensional stability and mechanical properties.

The zeta potentials of ZrP, OZrP, ZnO NPs, and ZCO-2 were determined at pH 8. The zeta potentials of the prepared samples were -40.5, -27.9, +3.5, and +9.5 mV, respectively. The results indicate that the surface charge of ZrP increased to more positive values with the addition of CTAB, COS, and ZnO NPs compared to unmodified samples. These changes in the surface potential of particles were mainly due to the intercalation of positively-charged quaternary ammonium compounds on the surface and the interlayer of ZrP. It was also found that the negatively-charged fibers interacted with the positively-charged ZCO particle *via* van der Waals forces.

Coating Morphology of Paper

The surface microstructure of the coated papers was studied to understand how the ZCO NCs coating enhanced the paper's antibacterial activity and improved the physical properties. The morphological structure of the control sample exhibited natural folds running parallel to the fiber's axis. The fiber's surface might be described as a smooth surface with normal structure (Fig. 5a and 5b). The ZCO NCs were not observed on the surface of the unmodified paper. Figures 5c-f depict the SEM imaging of the antibacterial paper treated with a 2.0 wt% of ZCO-1 and ZCO-2 NCs. Figure 5c shows that the regular-shaped, ZCO-1 NCs were attached to the fiber's surface. High magnification SEM images showed the existence of ZCO-1, as depicted in Fig. 5d. Figure 5d clearly shows that the ZCO-1 NCs were evenly distributed on the fiber's surface or between the fibers, and the size of those particles varied slightly. Similarly, as shown in Fig. 5e and 5f, more ZCO-2 NCs were present on the fiber's surface, which were produced using the surface coating method. The results indicated that ZCO NCs was round and adhered evenly on the surface of the paper fiber due to the physi-sorption and ionic bonding.

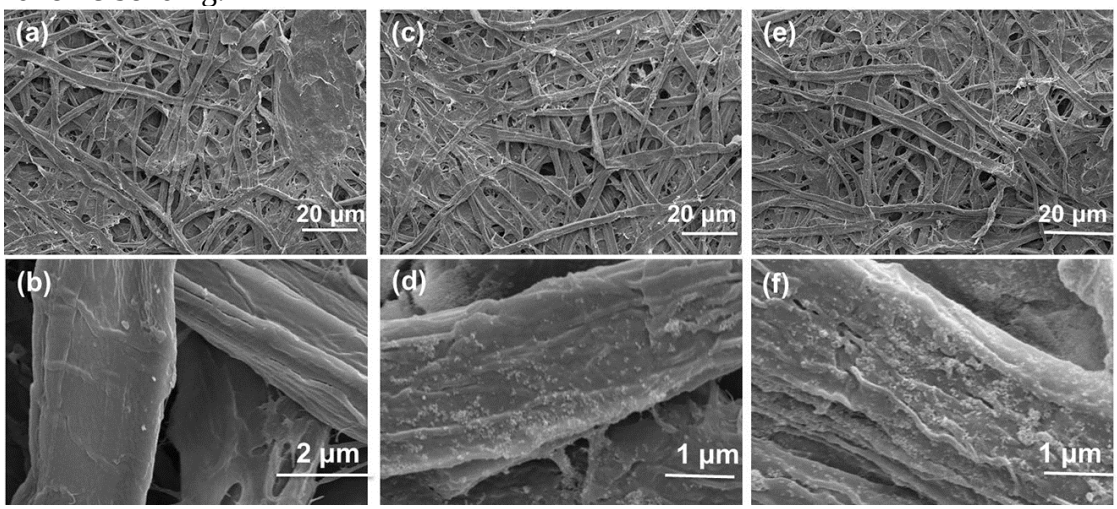

Fig. 5. SEM images of finished paper: (a, b) control; (c, d) ZCO-1 (2.0 wt%); (e, f) ZCO-2 (2 wt%)

Antibacterial Activity

Antibacterial activity is a very important characteristic of packaging paper. Both ZnO and COS are reported as efficient antibacterial agents (Vasile *et al.* 2014). The ZnO NPs were distributed on and intercalated into the interlayer of OZrP and blended with COS to form the composite that was applied as the coating agent. The ZCO-2 NPs were coated on paper sheets, and was tested using the zone of inhibition method. The photographs of the inhibition zone of the antibacterial papers and their values are shown in Fig. 6 and Table 1, respectively.

Figure 6 showed no clear zone of inhibition observable around the control paper. By contrast, the presence of ZCO-2 NCs on the paper's surface inhibited the bacterial growth and exhibited a clear zone of inhibition. As shown in Fig. 6a, the diameter of the inhibition zone for the ZCO-2 NCs-coated paper against *S. aureus* increased from 5.2 to 11.8 mm. Compared with the other three bacterial species, *E. coli* had the poorest sensitivity to the antibacterial paper, as shown in Fig. 6b. This may be because of the differences in cell wall structure and composition. The finished papers, with ZCO-2 NCs showed good antimicrobial properties, as shown in Fig. 6c and 6d. This was mainly attributed to the large number of ZnO NPs. Therefore, it has been proposed that the ZnO NPs could attach to the bacterial cell wall through electrostatic interaction, rupture the cell walls, increase the permeability, cause the leakage of cytoplasm, and lead to bacterial cell death (Gordon *et al.* 2011). Furthermore, the water-soluble COS could react with glycoprotein in the cell wall, change the permeability of cell membrane, and disrupt the normal physiological activity of cell membrane (Liu *et al.* 2014). Therefore, with the help of the synergistic antimicrobial capacity of COS and ZnO NP, the finished paper, with ZCO-2 NCs, exhibited satisfactory antibacterial activity.

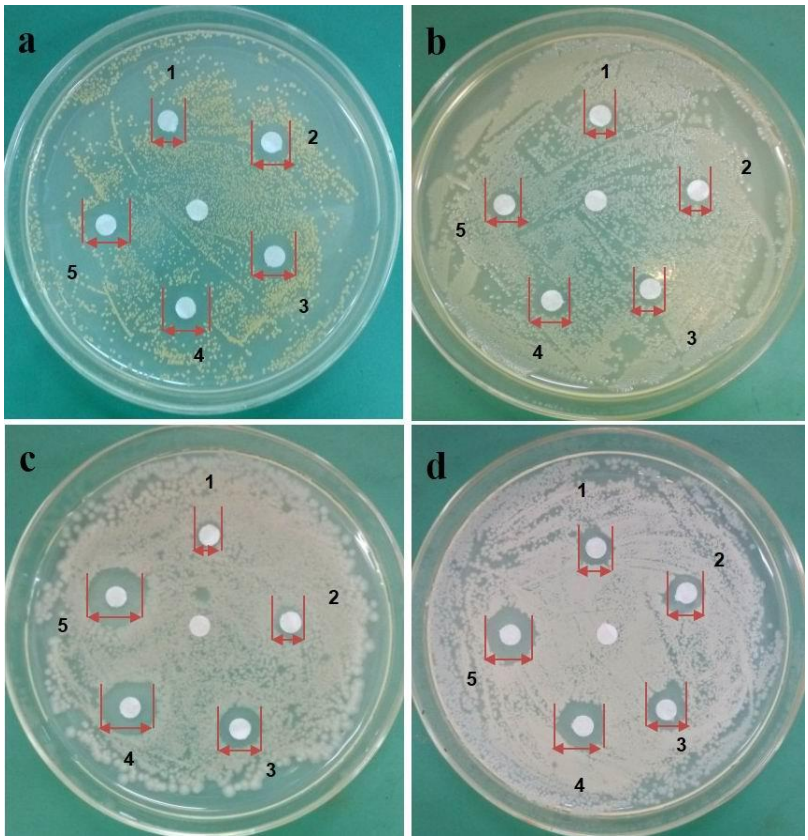

Fig. 6. Antibacterial effects of the finished papers: (a) *Staphylococcus aureus*; (b) *Escherichia coli*; (c) *Aspergillus niger*; (d) *Bacillus subtilis*; (1) 0.79%, (2) 1.8%, (3) 2.68%, (4) 3.92%, (5) 4.86% (wt%)

Table 1. Antibacterial Inhibition Zone of the Finished Paper

Antibacterial, ZCO-2-coated paper with varying ZCO-2 concentrations (wt%)	Inhibition zone of tested microorganisms (mm)			
	Staphylococcus aureus	*Escherichia coli*	*Aspergillus niger*	*Bacillus subtilis*
blank	0	0	0	0
0.79	4.20 ±0.48	2.64 ±0.60	3.88 ±1.53	5.36 ±1.21
1.87	6.22 ±0.43	3.54 ±0.88	4.72 ±0.40	6.24 ±0.89
2.68	8.34 ±0.78	4.22 ±1.51	8.20 ±1.47	8.84 ±1.40
3.92	10.64 ±1.20	5.14 ±1.24	11.84 ±0.55	10.86 ±1.66
4.86	11.88 ±1.49	5.60 ±1.29	13.20 ±1.43	12.62 ±1.47

Data reported as the mean ± standard deviation

Influence of ZCO NCs on the Physical Properties of Paper

In addition to antimicrobial activity, physical properties were also considered for packaging paper. Figure 7 shows the brightness, tensile, tear, and bursting properties of modified paper with different ZCO-2 NCs concentrations.

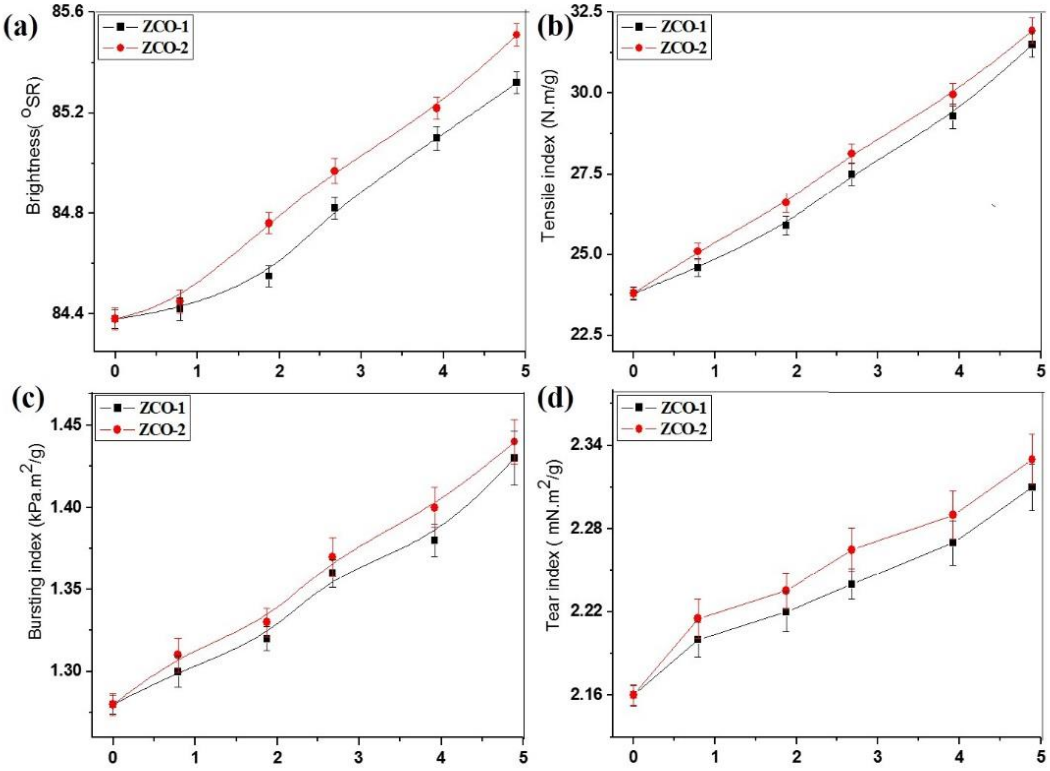

Fig. 7. Physical properties of the finished paper with different ZCO NC concentrations. Data are reported as the mean ± standard deviation

As shown in Fig. 7a, antibacterial papers coated with ZCO NCs exhibited an improvement in brightness (1.1 to 1.3%), compared to the control papers. The brightness of the antibacterial paper increased with increasing ZCO NC concentrations. The small particle size of the prepared ZCO NCs resulted in a change in the geometry of the pores, which affected the optical properties of the coated paper and increased the paper brightness compared to the control papers. Figure 7b shows the tensile strength of antibacterial papers. The tensile strength of antibacterial paper increased from 23.8 to 31.9 Nm/g with the increase of antibacterial agent concentration. The paper's tensile strength increased by 36.9% when the dosage of ZCO-2 was 2.0 wt%. As shown in Fig. 7c, the bursting index of the antibacterial paper increased, with increasing ZCO-2 NC concentrations. Furthermore, Fig. 7d indicates that the tear index of the coated paper was enhanced compared to the control, at 2.16 KPa.m^2/g.

CONCLUSIONS

1. A novel, multifunctional coating agent, based on ZnO NPs, COS, and OZrP NCs, was prepared in an environmentally friendly one-pot approach and was applied to paper to impart favorable antibacterial properties.
2. The morphology of the prepared ZnO NPs was polyhedron, and the average particle diameter was less than 50 nm. The COS was incorporated into the interlayer of OZrP and ZnO NPs was well dispersed on the surface and internally by the electrostatic assembly.
3. The presence of ZCO NCs positively affected the physical properties of the finished papers. The finished papers with the ZCOZ NCs exhibited good antimicrobial properties, which suggested that the novel antibacterial paper modified can be applied to packaging materials.

ACKNOWLEDGMENTS

This work was financially supported by the support of the National Key Technology R&D Program (2013BAC01B03)

REFERENCES CITED

Anandhavelu, S., and Thambidurai, S. (2011). "Preparation of chitosan–zinc oxide complex during chitin deacetylation," *Carbohydrate Polymers* 83(4), 1565-1569. DOI: 10.1016/j.carbpol.2010.10.006

Chan, Y., Huang, C., Ou, K., and Peng, P. (2011). "Mechanical properties and antibacterial activity of copper doped diamond-like carbon films," *Surface & Coatings Technology* 206(6), 1037-1040. DOI: 10.1016/j.surfcoat. 2011.07. 034

Fu, F., Li, L., Liu, L., Cai, J., Zhang, Y., Zhou, J., and Zhang, L. (2015). "Construction of cellulose based ZnO nanocomposite films with antibacterial properties through one-step coagulation," *ACS Applied Materials & Interfaces* 7, 2597-2606. DOI: 10.1021/am507639b

Gordon, T., Perlstein, B., Houbara, O., Felner, I., Banin, E., and Margel, S. (2011). "Synthesis and characterization of zinc/iron oxide composite nanoparticles and their antibacterial properties," *Colloids and Surfaces A: Physicochemical and Engineering Aspects* 374(1-3), 1-8. DOI: 10.1016/j.colsurfa.2010.10.015

Hubbe, M. A., and Bowden, C. (2009). "Handmade paper: A review of its history, craft, and science," *BioResources* 4(4), 1736-1792. DOI: 10.15376/biores.4.4. 1736-1792.

ISO 1924. (2008). "Paper and Board-Determination of tensile properties - Part 2: Constant rate of elongation method (20 mm/min)," International Organization for Standardization, Geneva, Switzerland.

ISO 1974. (2012). "Paper-Determination of tearing resistance - Elmendorf method," International Organization for Standardization, Geneva, Switzerland.

ISO 2758. (2001). "Paper-Determination of bursting strength," International Organization for Standardization, Geneva, Switzerland.

Liu, X., Xia, W., Jiang, Q., Xu, Y., and Yu, P. (2014). "Synthesis, characterization, and antimicrobial activity of kojic acid grafted chitosan oligosaccharide," *Journal of Agricultural and Food Chemistry* 62(1), 297-303. DOI: 10.1021/jf404026f

Krishna Rao. K. S. V., Ramasubba Reddy, P., Lee, Y.-I., and Kim, C. (2012). "Synthesis and characterization of chitosan–PEG–Ag nanocomposites for antimicrobial application," *Carbohydrate Polymers* 87(1), 920-925. DOI: 10.1016/j.carbpol.2011.07.028

Liu, K., Lin, X., Chen, L., Huang, L., Cao, S., and Wang, H. (2013). "Preparation of microfibrillated cellulose/chitosan-benzalkonium chloride biocomposite for enhancing antibacterium and strength of sodium alginate films," *Journal of Agricultural and Food Chemistry* 61(26), 6562-6567. DOI: 10.1021/jf4010065

Liu, K., Xu, Y., Lin, X., Chen, L., Huang, L., Cao, S., and Li, J. (2014). "Synergistic effects of guanidine-grafted CMC on enhancing antimicrobial activity and dry strength of paper," *Carbohydrate Polymer* 110, 382-387. DOI: 10.1016/j. carbpol.2014.03.086

Diez-Pascual, A. M., and Diez-Vicente, A. L. (2014). "Development of nanocomposites reinforced with carboxylated poly(ether ether ketone) grafted to zinc oxide with superior antibacterial properties," *ACS Applied Materials & Interfaces* 6, 3729-3741. DOI: 10.1021/am500171x

Lu, Y., Shah, A., Hunter, R. A., Soto, R. J., and Schoenfisch, M. H. (2015). "S-Nitrosothiol-modified nitric oxide-releasing chitosan oligosaccharides as antibacterial agents," *Acta Biomaterialia* 12, 62-69. DOI: 10.1016/j.actbio. 2014.10.028

Maclachian, D. J., and Morgan, K. R. (1992). "Phosphorus-31 solid-state NMR studies of the structure of amine-intercalated alpha-zirconium phosphate 2 titration of alpha-zirconium phosphate with n-propylamine and n-butylamine," *Journal of Chemical Physics* 96, 3458-3464. DOI: 10.1021/j100187a053

Manna, J., Goswami, S., Shilpa, N., Sahu, N., and Rana, R. K. (2015). "Biomimetic method to assemble nanostructured Ag@ZnO on cotton fabrics: application as self-cleaning flexible materials with visible-light photocatalysis and antibacterial activities," *ACS Applied Materials & Interfaces* 7, 8076-8082. DOI: 10.1021/acsami.5b00633

Nassar, M. A., and Youssef, A. M. (2012). "Mechanical and antibacterial properties of recycled carton paper coated by PS/Ag nanocomposites for packaging," *Carbohydrate Polymer* 89(1), 269-274. DOI: 10.1016/j.carbpol.2012.03.007

Shah, A. H., Basheer Ahamed, M., Neena, D., Mohmed, F., and Iqbal, A. (2014). "Investigations of optical, structural and antibacterial properties of Al-Cr dual-doped ZnO nanostructures," *Journal of Alloys and Compounds* 606, 164-170. DOI: 10.1016/j.jallcom.2014.04.040

Sun, T., Hao, H., Hao, W. T., Yi, S. M., Li, X. P., and Li, J. R. (2014). "Preparation and antibacterial properties of titanium-doped ZnO from different zinc salts," *Nanoscale Research Letter* 9(1), 98. DOI: 10.1186/1556-276X-9-98

TAPPI T205 sp-02. (2002). "Forming handsheets for physical tests of pulp," *TAPPI Press*, Atlanta, GA.

TAPPI T452. (1998). "Brightness of pulp, paper and paperboard (directional reflectance at 457 nm)," *TAPPI Press*, Atlanta, GA.

Vasile, B. S., Oprea, O., Voicu, G., Ficai, A., Andronescu, E., Teodorescu, A., and Holban, A. (2014). "Synthesis and characterization of a novel controlled release zinc oxide/gentamicin-chitosan composite with potential applications in wounds care," *International Journal of Pharmaceutics* 463(2), 161-169. DOI: 10.1016/j.ijpharm.2013.11.035

Wu, S., Zhang, Z., Wang, Y., Liao, L., and Zhang, J. (2014). "Influence of montmorillonites exchange capacity on the basal spacing of cation-anion organo-montmorillonites," *Materials Research Bulletin* 59, 59-64. DOI: 10.1016/j.materresbull.2014.06.007

Wu, Z., Zhang, L., Guan, Q., Ning, P., and Ye, D. (2014). "Preparation of α-zirconium phosphate-pillared reduced graphene oxide with increased adsorption towards methylene blue," *Chemical Engineering Journal* 258, 77-84. DOI: 10.1016/ j.cej.2014.07.064

Article submitted: April 2, 2015; Peer review completed: June 29, 2015; Revised version received: July 17, 2015; Further revision: July 20, 2015; Accepted: July 22, 2015; Published: August 3, 2015.
DOI: 10.15376/biores.10.3.6001-6013